

Investigation of Bias-Temperature Instability in work-function-tuned high- k /metal-gate stacks

B. Kaczer,^{a)} A. Veloso, and Ph. J. Roussel
IMEC, B-3001 Leuven, Belgium

T. Grasser
Christian Doppler Laboratory for TCAD at the Institute for Microelectronics, TU Wien, A-1040 Vienna, Austria

G. Groeseneken
IMEC, B-3001 Leuven, Belgium and ESAT Department, KU Leuven, B-3001 Heverlee, Belgium

(Received 8 June 2008; accepted 17 November 2008; published 9 February 2009)

The impact of V_{th} -adjusting layers on high- k /metal-gate n - and p FinFET V_{th} stability is investigated. Additional insight is gained by monitoring ΔV_{th} recovery transients over several decades in time. V_{th} -adjusting capping layers deposited directly on top of the gate dielectric degrade the V_{th} stability. The V_{th} stability improves as the capping layers are buried in the gate metal and are thus isolated from the gate dielectric. A combination of a capping layer thickness and depth in the metal gate is found that practically eliminates n FET V_{th} instability. © 2009 American Vacuum Society. [DOI: 10.1116/1.3054352]

I. INTRODUCTION

The introduction of high- k /metal-gate stacks into complementary metal-oxide semiconductor (CMOS) technology requires separately “tuning” the gate work function for n - and p FET devices. Adjustment of the field-effect transistor (FET) threshold voltage V_{th} can be achieved, e.g., by insertion of “capping” layers into the gate stack, as discussed elsewhere.¹ In this work we investigate the impact of these layers on the bias-temperature instability (BTI) of V_{th} in n - and p FinFETs with HfSiO dielectrics and TiN gates. An extension of a standard BTI evaluation technique² allows us to monitor V_{th} transients and thus to better understand and compare the influence of the layers.

We find that capping layers deposited directly on top of the gate dielectric degrade the V_{th} stability. Conversely, p FET capping layers separated sufficiently from the gate dielectric, i.e., “buried” in the gate metal, have V_{th} stability identical to reference stacks. Similarly, the n FET V_{th} stability improves as the capping layers are isolated from the gate dielectric. Finally, we report that a capping layer suitably spaced from the gate dielectric *practically eliminates* n FET V_{th} instability.

II. SAMPLES

Silicon-on-insulator (SOI) n - and p FinFETs with $L_{FIN} = 1 \mu\text{m}$, $W_{FIN} = 10 \times 1 \mu\text{m}$, and $H_{FIN} = 65 \text{ nm}$ were used. AlO and DyO capping layers were, respectively, introduced into the p FET and n FET stacks, resulting in V_{th} and capacitance equivalent thickness (CET) as given in Fig. 1.¹ Conservative dielectrics thicknesses were chosen to avoid reliability issues not related to negative and positive BTI (NBTI and PBTI). The completed stacks were exposed to 1050 °C during FET junction formation.

^{a)}Electronic mail: kaczer@imec.be

III. MEASUREMENT TECHNIQUE

The BTI is typically assessed using the measure-stress-measure (MSM) technique,² during which the threshold voltage shift ΔV_{th} with respect to the initial V_{th} is measured after each stress phase. Such evaluation tacitly assumes a *time-independent* ΔV_{th} , while in reality strong transients are observed.² The V_{th} relaxation *trends* thus carry additional information about the BTI processes in the studied device, which is otherwise lost in the single- V_{th} MSM measurements.

Here we therefore use the recently introduced *extended* MSM (eMSM) technique (Ref. 2) to monitor the relaxation transients after each stress phase [Fig. 2(a)]. Since the BTI relaxation typically occurs over many time scales, the transients are recorded and plotted on the logarithmic time scale from $\sim 1 \text{ ms}$ to $\sim 10 \text{ s}$, i.e., over four decades in time. An example of such plot is shown in Fig. 2(b), with the time t_{relax} always measured from the end of the preceding stress phase. The last relaxation transient is typically monitored up to 3–10 ks, i.e., over $6\frac{1}{2}$ –7 decades in time.

All measurements are done at temperature $T = 125 \text{ °C}$. The measurement voltage V_{meas} [Fig. 2(a)] is chosen close to the initial threshold voltage $V_{th,initial}$ (Fig. 1).³ The stress voltages V_{stress} are chosen with respect to $V_{th,initial}$, and the observations are therefore reported at the “overdrive” voltage $V_{s-th} = V_{stress} - V_{th,initial}$. The integrity of the gate dielectric after the entire MSM sequence is checked by assessing the gate leakage at V_{meas} .²

IV. PFET RESULTS (NBTI)

In all the p FET high- k stacks studied, ΔV_{th} transients show a behavior qualitatively identical to what we previously observed on conventional SiO₂ and SiON stacks, with the $\log(t_{relax})$ -like relaxation [Fig. 2(b)], indicating an underlying dispersive process.^{4,5} Following the same analysis as in

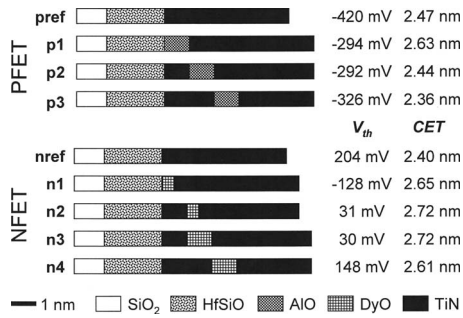


FIG. 1. Investigated *p*- and *n*FinFET gate stacks. All film thicknesses are to the scale indicated in the figure. Capping layers at different positions in gate stacks adjust V_{th} and slightly influence CET.

Ref. 5, assuming *universality of relaxation*,⁶ we quantify the ΔV_{th} transients [Fig. 2(b)] by separating them into the relaxing (“recoverable” or “*R*”) and the permanent (“unrecoverable” or “*P*”) degradation components, i.e., $\Delta V_{th} = R + P$. With the above assumption, we describe the recoverable component *R* by the universal relaxation function in the following form:

$$R(t_{stress}, t_{relax}) = \frac{R(t_{stress}, t_{relax} = 0)}{1 + B\xi^\beta}, \quad (1)$$

where $\xi = t_{relax}/t_{stress}$ is the *universal* (dimensionless) relaxation time, t_{stress} is the *total (cumulative)* stress time, and *B* is a scaling parameter. The functional form of Eq. (1) has properties similar to a stretched exponential, which is often in-

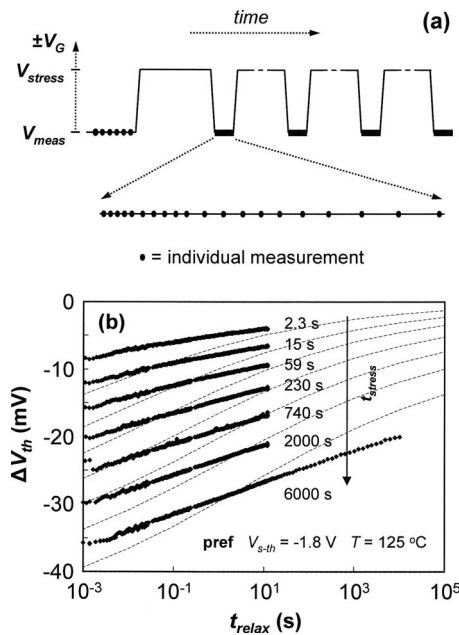


FIG. 2. (a) Extended MSM stress/relaxation voltage sequence applied at FET gate. The FET source current is monitored at V_{meas} after each stress phase and converted to ΔV_{th} relaxation transient spanning several decades. (b) $\Delta V_{th} < 0$ V transients at increasing cumulative stress times measured on stack “pref” (symbols). ΔV_{th} transients calculated by fitting relaxation data obtained on 1.4 nm SiON *p*FET stressed at similar oxide electric field (Ref. 5) are shown for comparison (dashed lines).

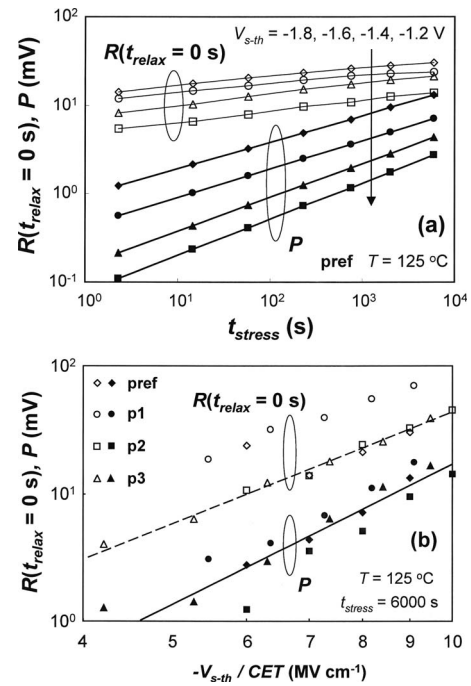


FIG. 3. (a) Permanent *P* and recoverable *R* components extracted from Fig. 2(b) (and other V_{stress} values on stack “pref”) vs t_{stress} . Unlike in Ref. 5, a simple power-law dependence on t_{stress} is assumed for the permanent component during extraction. (b) Extracted *P* and *R* components at $t_{stress} = 6000$ s for all studied *p*FET stacks. Stacks with buried capping layers (“p2” and “p3”) behave identically to the reference stack “pref” (spread in the *P* component data is within the precision of the extraction technique).

voked to describe the relaxation of dispersive systems, and β has the attributes of a dispersion parameter.⁴

The recoverable component *R* is reported at $t_{relax} = 0$ s, i.e., the moment *immediately* after the removal of stress gate voltage. The permanent component $P(t_{stress})$ reported here then represents the remaining ΔV_{th} after the full relaxation of the recoverable component, corresponding to $t_{relax} = \infty$ s in Eq. (1) (the possibility of long-term recovery of the *P* component is discussed in Ref. 7). The result of this extrapolation, done after each stress phase (i.e., as a function of the total t_{stress}) and for each stress voltage condition, is shown in Fig. 3(a).

As NBTI is typically assumed to be accelerated by the electric field at the substrate/dielectric interface,⁸ both components are compared at V_{s-th}/CET . In order to reduce measurement and extraction inaccuracies, the comparison is done at the maximum degradation at $t_{stress} = 6000$ s. The comparison of all *p*FET stacks in Fig. 3(b) shows that the permanent degradation is identical for all *p*FET stacks, irrespective of the capping layer presence or its position. In stacks “p2” and “p3,” where the capping layer is buried in the gate electrode, the recoverable component behaves identically to the reference.

Interestingly, the recoverable component increases considerably in stack “p1,” which coincides with significant mobility degradation observed in the *p*FETs with this stack.¹ Both effects are most probably due to new states created by outdiffusion of Al, likely as far as the SiO₂ interfacial layer.

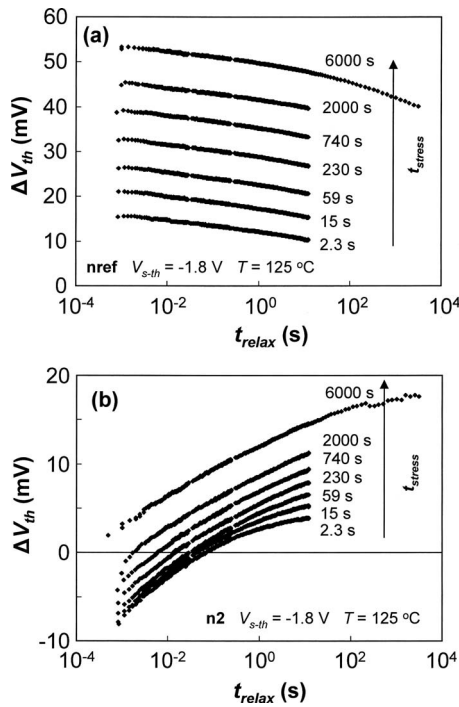


FIG. 4. (a) Relaxation of $\Delta V_{th} > 0$ V due to negative charge in reference *n*FET stack and (b) opposite trend due to insertion of DyO is superimposed on the overall positive shift in ΔV_{th} with increasing stress, same as in (a).

In stacks *p*2 and *p*3 the TiN barrier prevents intermixing of Al during the high-temperature junction formation, which preserves the NBTI behavior seen in the reference stack.

We have already noted that although the studied *p*FET devices contain a high-permittivity gate dielectric layer, their NBTI relaxation behavior is comparable to “conventional” SiO₂ and SiON *p*FETs. This similarity is not only qualitative but also quantitative. The relaxation dispersion is very similar in both types of stacks—the dispersion parameter β is typically between 0.12 and 0.16 in the high-*k* stacks discussed here, while ~ 0.16 was found for SiON *p*FETs.⁵ Also the magnitude of both components is comparable to the conventional *p*FET, as is documented in Fig. 2(b). This is an indication of a similar NBTI mechanism in both the conventional and the high-*k* *p*FETs, controlled by the properties of the oxide close to the substrate/dielectrics interface.⁹

V. NFET RESULTS (PBTI)

In *n*FETs with the reference gate stack “nref” following positive BTI stress, ΔV_{th} transients of the opposite polarity (i.e., corresponding to negative charge) are observed in Fig. 4(a).¹⁰ Note that PBTI stress again results in very long, $\log(t_{relax})$ -like ΔV_{th} relaxation transients, just like those typically observed in the NBTI/*p*FET case [Fig. 2(b)].

In the stacks with the DyO capping layer, the ΔV_{th} transients reveal an *additional* mechanism corresponding to positive charging [Fig. 4(b)].¹¹ Note that the existence of the two “competing” components would be completely overlooked if only a traditional single-point MSM technique were used.⁴ The presence of the two transient components in stacks

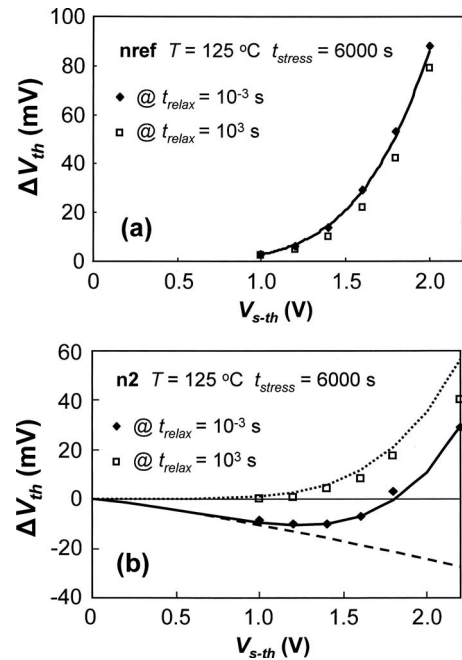


FIG. 5. (a) In the *n*FET reference stack, ΔV_{th} at $t_{relax} = 10^{-3}$ s vs V_{s-th} can be fitted with $\sim V_{s-th}^2$. (b) ΔV_{th} at 10^{-3} s in stack “n2” can be fitted with two competing trends (respectively, proportional to V_{s-th}^2 and $-V_{s-th}^{1.5}$). Stacks *n*2 and “n3” behave similarly.

“n1”–“n4,” however, precludes the use of the analysis based on relaxation universality (cf. Sec. IV). We therefore evaluate ΔV_{th} at the shortest and longest relaxation times as a function of V_{s-th} (Fig. 5). The reference stack positive ΔV_{th} appears to follow the power-law dependence on V_{s-th} [Fig. 5(a)]. In contrast to that, ΔV_{th} at 10^{-3} s in stacks “n2” and “n3” changes from negative to positive as V_{s-th} is increased. This trend can be reproduced with two opposite components, both depending on V_{s-th} [Fig. 5(b)]. The fit representing the positive component (dotted line) tracks ΔV_{th} at 10^3 s, suggesting the negative transient abating after 10^3 s.

While depositing the DyO layer directly on top of the dielectric (stack *n*1) leads to large instabilities and *n*FET mobility degradation¹ likely due to intermixing of the layers, separating the DyO layer by the gate metal substantially reduces outdiffusion of Dy and, in fact, improves the V_{th} sta-

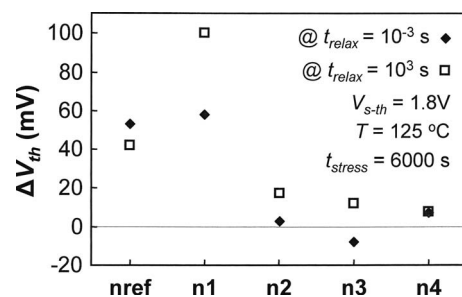


FIG. 6. Depositing the DyO layer directly on top of the dielectric (stack “n1”) aggravates the V_{th} instability over the reference stack “nref,” while burying the DyO layer in the gate metal (stacks “n2”—“n4”) substantially improves it.

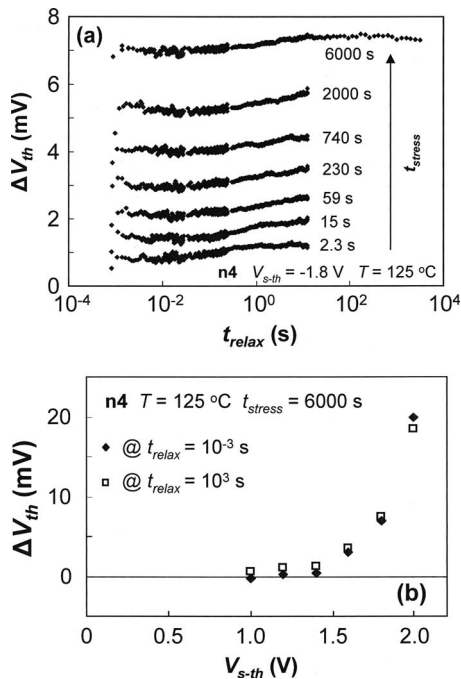


FIG. 7. (a) In stack “*n4*,” the two components in ΔV_{th} transients appear to be compensating, with minute overall ΔV_{th} shift. (b) At $V_{s-th}=1$ V, the overall ΔV_{th} after 6000 s of stress is ~ 1 mV.

bility with respect to the reference stack, as shown in Fig. 6. Most notably, in stack *n4* with the DyO layer separated by 2 nm of TiN, after 6000 s of $T=125$ °C and $V_{s-th}=1.8$ V stress, ΔV_{th} is mere 7 mV and stable, as is also documented by Fig. 7(a). This *n*FET high-*k*/metal gate stack shows extremely small instability, of the order of 1 mV or less at $V_{s-th}=1$ V [Fig. 7(b)]. A similarly negligible instability can be expected at operating conditions ($V_{s-th}\approx 0.6-0.8$ V and 3×10^8 s). We speculate that this extremely stable V_{th} could be due to compensation of defect states in the dielectric by Dy.

VI. CONCLUSIONS

The impact of V_{th} -adjusting layers on high-*k*/metal-gate *n*- and *p*FinFETs V_{th} stability is investigated. Additional insight is gained by application of the recently developed extended MSM technique to monitor ΔV_{th} transients. Capping layers deposited directly on top of the gate dielectric degrade the V_{th} stability, most probably due to new states created by intermixing of the capping layer with the dielectric. V_{th} stability improves as the capping layers are buried in the gate metal, thus reducing their outdiffusion into the gate dielectric. A combination of a capping layer thickness and depth in the metal gate is found that hugely improves *n*FET V_{th} stability.

¹A. Veloso *et al.*, Proceedings of the 2008 International Symposium on VLSI Technology (IEEE, Piscataway, NJ, 2008), p. 14.

²B. Kaczer, T. Grasser, Ph. J. Roussel, J. Martin-Martinez, R. O’Connor, B. J. O’Sullivan, and G. Groeseneken, Proceedings of the 2008 IEEE International Reliability Physics Symposium, 2008 (IEEE, Piscataway, NJ, 2008), p. 20.

³T. Grasser, P.-J. Wagner, Ph. Hehenberger, W. Gös, and B. Kaczer, Proceedings of the 2007 International Integrated Reliability Workshop, 2007 (IEEE, Piscataway, NJ, 2007), p. 6.

⁴B. Kaczer, V. Arkhipov, R. Degraeve, N. Collaert, G. Groeseneken, and M. Goodwin, Proceedings of the 2005 IEEE International Reliability Physics Symposium, 2005 (IEEE, Piscataway, NJ, 2005), p. 381.

⁵T. Grasser, B. Kaczer, P. Hehenberger, W. Gös, R. O’Connor, H. Reisinger, W. Gustin, and C. Schlünder, Proceedings of the 2007 International Electron Devices Meeting, 2007 (IEEE, Piscataway, NJ, 2007), p. 801.

⁶M. Denais *et al.*, Proceedings of the 2006 IEEE International Reliability Physics Symposium, 2006 (IEEE, Piscataway, NJ, 2006), p. 735.

⁷T. Grasser, B. Kaczer, and W. Gös, Proceedings of the 2008 IEEE International Reliability Symposium, 2008 (IEEE, Piscataway, NJ, 2008), p. 28.

⁸A. E. Islam, H. Kufluoglu, D. Varghese, S. Mahapatra, and M. A. Alam, IEEE Trans. Electron Devices **54**, 2143 (2007).

⁹S. Zafar (private communication).

¹⁰D. Heh, C. D. Young, and G. Bersuker, IEEE Electron Device Lett. **29**, 180 (2008).

¹¹S. Z. Chang *et al.*, Proceedings of the 2008 International Symposium on VLSI Technology (IEEE, Piscataway, NJ, 2008), p. 62.